Journal of Solid State Chemistry 182 (2009) 3183–3187

Contents lists available at ScienceDirect

Journal of Solid State Chemistry

journal homepage: www.elsevier.com/locate/jssc

Electronic structure and magnetic properties of $RuFe_3N$ nitride

A.V. dos Santos [a,*], C.A. Kuhnen [b]

[a] Departamento de Ciências Exatas e da Terra URI (DCET-URI), Av. Universidade das Missões, 464, 98892-98470 Santo Ângelo, RS, Brazil
[b] Departamento de Física, UFSC, 88040-900 Florianópolis, SC, Brazil

ARTICLE INFO

Article history:
Received 18 May 2009
Received in revised form
17 July 2009
Accepted 27 July 2009
Available online 7 August 2009

Keywords:
Perovskite nitrides
Electronic structure
Magnetic properties
Hyperfine parameters

ABSTRACT

Self-consistent band structure calculations were performed on nitride $RuFe_3N$ in order to investigate its magnetic and ground state properties. The Linear Muffin-Tin Orbital (LMTO) method was employed and calculations were performed at several lattice parameters so as to obtain the $RuFe_3N$ equilibrium volume. Nonmagnetic and ferromagnetic LMTO calculations have shown that the $RuFe_3N$ stable stage is ferromagnetic with constant lattice equilibrium of 7.2502 atomic units (a.u.). At equilibrium volume the LMTO calculations have given magnetic moments of 1.25 and 1.63 μ_B at Ru and Fe sites, respectively, and no magnetic moment at N sites. The analysis of states density at equilibrium volume as well as the results for charge transfer illustrates why this ruthenium nitride is ferromagnetic. The LMTO calculations anticipate that the magnetic moment, the hyperfine field (the Fermi contact) and the isomer shift show a strong dependence on the lattice spacing.

1. Introduction

In recent years the interest in researching new materials with specific physical properties has been reflected in the vast number of experimental and theoretical works carried out on electronic, magnetic and crystallographic properties of iron-based nitrides. Iron-based nitrides are very important due to their potential industrial applications and for that reason several experimental and theoretical works [1–17] have been carried out on their electronic, magnetic, mechanical and crystallographic properties. Likewise, it is known that iron-transition metal nitrides may be used as hard metals to make wear-resistant materials, and iron nitrides such as γ'-Fe_4N and α''-$Fe_{16}N_2$ are distinguished by their high saturation magnetization and low coercivity [10,11]. There is a wide range of papers dedicated to developing the alloy magnetic structure of the perovskite-nitride γ'-Fe_4N, which shows high coercive field [12–17].

The perovskite-nitride γ'-Fe_4N is fully ordered with a simple crystallographic structure. Moreover, it is a stable nitride with iron atoms occupying the corner (FeI) and the face-centered positions (FeII), and nitrogen atoms occupying the body-centered positions. It is known that few atoms can substitute iron atoms at the corner of the cube if their chemical affinity for nitrogen atoms is weaker than iron–nitrogen affinity. Chemical affinity between nitrogen and another metal atom increases if this atom is on the left side of iron in the periodic table. In spite of several experimental difficulties in obtaining ordered substituted iron nitrides, several ternary iron nitrides ($Fe_{1-x}Me_xFe_3N$) can be obtained by mechanical alloying, and the effects of different substitutions on $Fe_{1-x}Me_xFe_3N$ ternary perovskite nitrides (where Me = Fe, Ti, V, Cr, Mn, Au, Ag, Pd, Ni, Pt, Sn, In, Zn, Cu, Co, Al, Ru, Os, Ir) have been reported both theoretically and experimentally using Mössbauer spectroscopy, magnetometry, X-ray and neutron diffraction techniques [5–9,12–21]. In addition, atoms located on the right side of the iron in the periodic table can be used to replace iron in some iron nitrides in a controlled disposition, giving fully ordered compounds such as $PdFe_3N$, $AuFe_3N$, $PtFe_3N$ and $NiFe_3N$, since these atoms replace the iron at the corner position (zero nitrogen as the nearest neighbor).

Regarding ruthenium substitution, Mössbauer and magnetic measurements [7] in $Fe_{1-x}Ru_xFe_3N$ alloys (with $0.05 < x < 0.2$) it is suggested that Ru replaces Fe especially in FeI sites with no significant change in the lattice parameter relating the Fe_4N nitride. Magnetic measurements [7] on $Fe_{1-x}Ru_xFe_3N$ showed that there is a reduction in the saturation magnetization upon increasing the concentration of Ru. As for $x = 0.2$, the value acquired was 141 emu/g at 4.2 K, or 6.22 μ_B per unit cell [7]. The present work is an effort to understand the influence of ruthenium substitution on the γ'-Fe_4N electronic and magnetic properties through the calculation of the electronic structure of fully ordered $RuFe_3N$ nitride. The calculations were made by using the self-consistent Linear Muffin-Tin Orbital method (LMTO).

Linear Muffin-Tin Orbital calculations [22,23] within the atomic spheres approximation (LMTO-ASA) were performed in order to obtain the magnetic and electronic structures of $RuFe_3N$-ordered nitride. For these calculations the crystal structure of the compound was taken as a simple cube with five atoms in the unit cell. When Ru atoms occupy the corner sites, the Fe atoms are in

* Corresponding author.
E-mail address: vandao@urisan.tche.br (A.V. dos Santos).

0022-4596/$ - see front matter © 2009 Elsevier Inc. All rights reserved.
doi:10.1016/j.jssc.2009.07.061

the center of faces and the nitrogen atoms occupy sites in the center of the cube.

Spin-polarized LMTO calculations were performed using the Vosko–Wilk–Nusair parametrization [24] for the exchange-correlation energy of the electron gas, whereas for the nonmagnetic calculations the Hedin–Lundqvist parametrization was used [25]. Although our LMTO calculations were made without spin–orbit interaction, they included combined correction terms [23]. On fully ordered $RuFe_3N$ nitride the Wigner–Seitz spheres (S_i) around ruthenium and iron atoms were taken so that they were of an equal size. The Wigner–Seitz values were obtained using $4/3\pi\sum S_i^3 = a^3$ (where a is the lattice parameter). As for the nitrogen, we took $S_N = 0.5S_{Fe}$ for the three nitrides. For the nitrides the overlap between Ru (corner position) and Fe (face-centered position) muffin-tin spheres were $0.066a$, and between N spheres and Fe or V face-centered spheres $0.080a$. There was no overlap between Ru at corner position and N spheres. The one-electron potentials were obtained self-consistently using reciprocal space sums with 544 **k**-points. The self-consistent cycles were carried out until energy convergence was reached on a scale better than 0.5 mRy. The solutions of the Schrödinger equations use *s*, *p*, *d* and *f* LMTO base functions for metals (Fe, Ru), and *s*, *p* and *d* base functions for nitrogen. The densities of states (DOS) were calculated as a sum of delta functions and a fixed number of mesh points, and the energy window was divided into a 1500 points mesh.

2. Results and discussion

The employment of the LMTO total energy calculations method was made on several lattice parameters so as to obtain the equilibrium volume of the $RuFe_3N$ nitride. Fig. 1 shows the results of nonmagnetic (NM) and ferromagnetic (FM) calculations (relative total energies in Ry and lattice spacing in atomic units). These binding curves were obtained through an analytical fitting

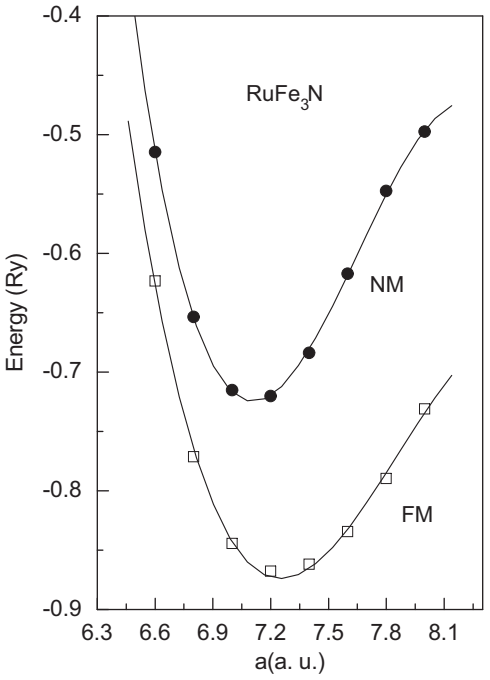

Fig. 1. Total energy curves (in Ry), versus lattice spacing (in atomic units) for the $RuFe_3N$ nitride. FM: ferromagnetic calculations; NM: nonmagnetic calculations (relative energies).

Table 1
Theoretical parameters for the $RuFe_3N$ nitride.

	ΔE (mRy)	a_{NM} (a.u.)	a_{FM} (a.u.)	B_{NM} (GPa)	B_{FM} (GPa)	P_c (kbar)
$RuFe_3N$ (Theor.)	29.96	7.1162	7.2502	296	214	172

Equilibrium lattice spacing a (in atomic units); bulk modulus B (in GPa); critical pressure in kbar.

of the calculated total energies to a third degree polynomial in each case. From Fig. 1 it is clear that the ferromagnetic state is the stable phase of the ordered $RuFe_3N$ nitride, according to the experimental results of $Fe_{1-x}Ru_xFe_3N$. Our calculation shows that the difference between the nonmagnetic total energy and ferromagnetic total energy at their respective equilibrium volumes ($\Delta E = E_{NM} - E_{FM}$) is ≈ 30 mRy per unit cell. Usually, the critical pressure at which a ferromagnetic material undergoes a transition to a NM state is defined as $P_c = -\Delta E/\Delta V$, where ΔE is per atom and ΔV is the difference between NM and FM equilibrium volumes. The critical pressure (P_c) definition was first employed by *P.* Mohn et al. [26] in his work on magneto-elastic anomalies in Fe–Ni Invar alloys, $NiFe_3N$ and $PdFe_3N$ nitrides [27]. We have also used this definition on the study of magnetic transition of inter-metallic bi-layers and substituted iron nitrides [28,29].

Table 1 shows the LMTO results for the equilibrium lattice parameters of NM and FM states as well as the respective bulk module and values of ΔE and P_c for the $RuFe_3N$. As a matter of comparison, there is an experimental critical pressure of Fe_4N obtained by forced magnetostriction measurements where we found 280 kbar [30], and the value [29] found through theoretical calculation was 430 kbar. For $PdFe_3N$ the theoretical values for P_c are 864 kbar [27] and 775 kbar [29], whereas for $MnFe_3N$ and $SnFe_3N$ the P_c values are 263 and 621 kbar, respectively [29]. The values of P_c are a feature of Invar-like behavior [29–32] of such nitrides (in Invar alloys nonmagnetic low-volume states are easily accessible giving a negative thermal expansion coefficient around room temperature). As we will see later in the study of $RuFe_3N$ magnetism under pressure, this nitride also exhibits an Invar-like behavior.

The calculated lattice constant for FM $RuFe_3N$ (Table 1) indicates an expansion relative to the γ'-Fe_4N (experimental lattice constant $a = 7.1713$ a.u.), which is due to the slightly higher atomic volume of ruthenium atoms. In a recent full-potential LAPW calculation on $RuFe_3N$ PADUANI [20] obtained 7.18 a.u. as the equilibrium lattice spacing, which agrees with the experiments on $Fe_{1-x}Ru_xFe_3N$ [7] with small amount of Ru substitution, that is, where the maximum value of x is only 0.2. Furthermore, the present LMTO calculation gives an equilibrium volume for the ferromagnetic phase ($a = 7.2502$ a.u.) of $RuFe_3N$, which is close to the experimental lattice spacing of $PdFe_3N$ (7.2722 a.u.) in conformity with the fact that Ru and Pd atoms are second neighbors in the periodic table having near equal atomic radii. As shown in Table 1, the bulk modulus is visibly higher than the bulk modulus of bcc Fe (in theory 205 GPa and in experiment 173 GPa [33]).

Calculations were compared to previous ones by using LMTO in the Fe_4N structure and the theoretical result of 406 GPa [29] was obtained. The experimental result in the same structure provides 198 GPa [32]. The result obtained by using FPLAPW [34] is closer to the experimental one since 150 GPa was found.

Table 2 presents some theoretical parameters of the $RuFe_3N$ nitride with spin polarization at equilibrium volume. The

Table 2
Calculated parameters at equilibrium volume for the $RuFe_3N$ nitride.

a (a.u.)		μ (μ_B)	ΔQ (e)	H_{FC} (kG)	IS (mm/s)
7.25	Ru	1.25	0.69	−58.5	–
	Fe	1.63	−0.78	−158.9	0.502
	N	0.00	1.65	31.7	–
	$RuFe_3N$	6.14	–	–	–

ΔQ in electrons; isomer shift in mm/s; hyperfine fields in kG.

experimental value for γ′-Fe_4N is 8.8 μ_B per unit cell [7,35] and the magnetic moment per unit cell decreases due to the ruthenium substitution instead of Fe [7,35]. The present results is in accordance with the experimental value obtained for $Fe_{1-x}Ru_xFe_3N$ [7] where the magnetization is 6.2 μ_B per formula unit, considering $x = 0.2$.

The LMTO value for the magnetization of $RuFe_3N$ is close to the FPLAPW result [20], which is 6.39 μ_B. At Fe sites, the magnetic moment decreases according to the value of Fe atoms at the face-centered position on Fe_4N, which is 2.10 μ_B [10,34,36]. The calculated LMTO magnetic moments at various sites shown in Table 2 agree with the previous FPLAPW results [20], which are 0.68, 1.89 and 0.04 μ_B for Ru, Fe and N sites, respectively. As a result, ruthenium substitution gives the magnetic moment per unit a cell with the same order of other metallic substitution, e.g. 7.44 μ_B for $PdFe_3N$ [27,37]; 7.20 μ_B for $NiFe_3N$ [27]; 6.14 and 6.42 μ_B for $AgFe_3N$ and $AuFe_3N$ [15]; 7.76 μ_B for $PtFe_3N$[38] and 6.00 μ_B for $SnFe_3N$ [39]. Concerning charge transfer, Table 2 shows that Fe sites are the electron-acceptors whereas N sites, in LMTO calculations, lose a large amount of charge that occupies the unbalanced spin-up and spin-down d states at Fe sites, thus contributing for the lowering of the magnetic moment at these sites. The LMTO high values reported in Table 2 for the charge transfer may be explained by the fact that the calculated charge at each site depends strongly on the choice of the Wigner–Seitz spheres. In this work we have considered the Wigner–Seitz radius of the nitrogen spheres as $S_N = 0.5S_{Fe}$, that is, taking relatively small spheres around nitrogen atoms, and explaining the large charge transfer from the nitrogen to metal atoms. For example, previous LMTO calculations on V_4N [21] showed that if we increase the radius of nitrogen spheres from $S_N = 0.55S_V$ to $0.70S_V$, the charge transfer from nitrogen to vanadium sites varies linearly from −1.209 to −0.556. Such a change reveals the strong dependence of the charge transfer with the volume of the spheres around nitrogen atoms. We chose $S_N = 0.5S_{Fe}$ as this relation gives theoretical results, which are in accordance with experimental results for a series of nitrides studied earlier [15,17–19,21], and because the convergence of the calculations are more difficult to achieve for large nitrogen spheres, having no improvement in the calculation of physical quantities of interest (in many cases no convergence was achieved for $S_N = 0.75S_{Fe}$). For that reason, the results of the present calculations must be considered as showing the trends in the charge transfer in $RuFe_3N$. Certainly, this calculated charge transfer reflects the nitrogen–metal and metal–metal interactions whose specific details may be revealed, as it will be seen when analyzing the density of states.

The partial densities of states (PDOS) at theoretical equilibrium volume were obtained so as to investigate the trends of the chemical bonds in the $RuFe_3N$ nitride from an itinerant model point of view. The $RuFe_3N$, the s, p and d-DOS for both spin directions are shown in Fig. 2 for N sites. As it is seen, the s states at these sites are located in the energy space, at energy range −0.5 to −0.25 Ry, while p states are smeared out at a range 0.20–0.75 Ry

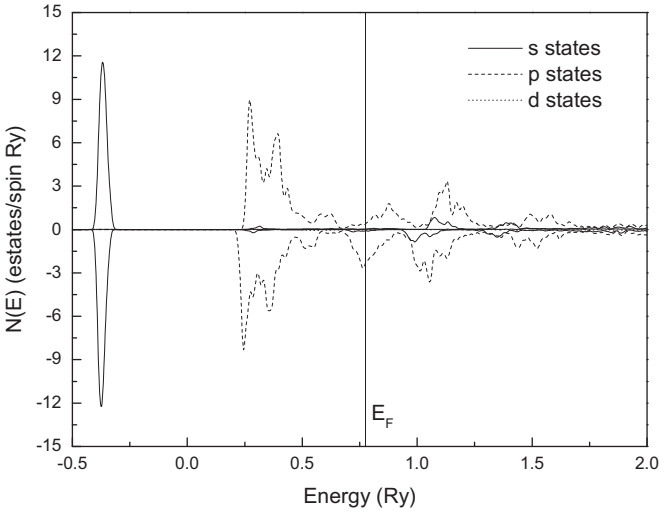

Fig. 2. The s, p and d-projected densities of states for spin-up and spin-down electrons at N sites of the $RuFe_3N$ nitride. E_F is the Fermi energy.

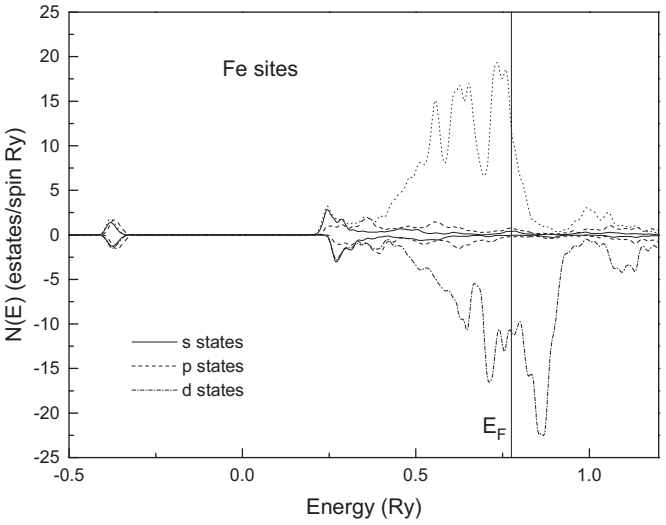

Fig. 3. The s, p and d-projected densities of states for spin-up and spin-down electrons at Fe sites of the $RuFe_3N$ nitride. E_F is the Fermi energy.

and, only a very small contribution from d states to the DOS is observed. The hybrid character of nitrogen states is not clearly defined as the curves of PDOS are not entirely smeared out in the energy space. For the Fe sites, the PDOS are shown in Fig. 3. Although the s-DOS and p-DOS are small, Fig. 3 shows the form of a structure in the DOS for s and p states (and also a small structure in the case of d states) at energy range −0.5 to −0.25 Ry reflecting the interactions of these states with those s states at N sites. For Fe (face-centered position) the interactions between N p states and Fe s states also appear as a pronounced peak in the s-DOS at Fe sites around 0.25 Ry. Thus, for $RuFe_3N$, as with Fe_4N and other nitrides ($MeFe_3N$ with Me = Sn, Pd, Au, Ag, Cu, Co, Zn), despite the strong interactions between N and Fe atoms at centered face positions, the spin-down d-states remain unoccupied giving a net magnetic moment on metal sites so that these nitrides are ferromagnetic. On the other hand, as opposed to the strong interactions between Fe and N atoms, the PDOS at Ru sites (Fig. 4) reveals that the interactions between

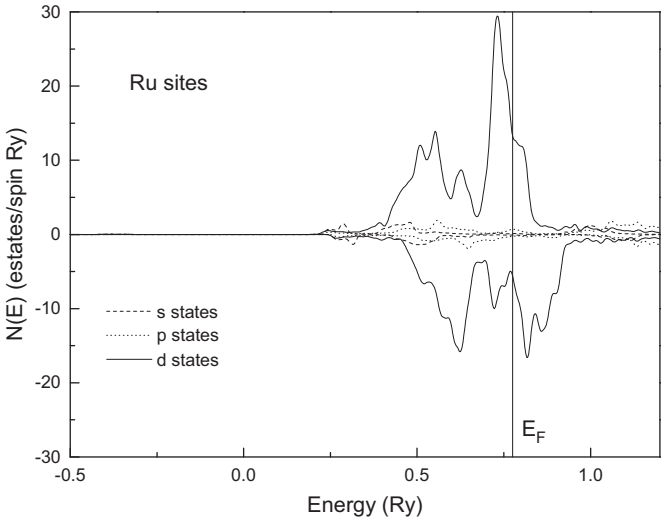

Fig. 4. The *s*, *p* and *d*-projected densities of states for spin-up and spin-down electrons at Ru sites of the $RuFe_3N$ nitride. E_F is the Fermi energy.

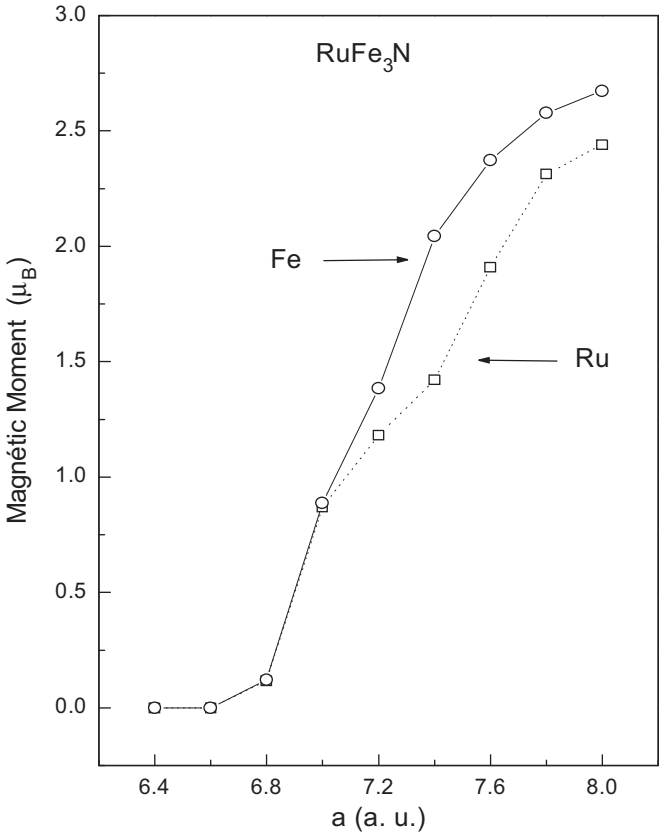

Fig. 5. The magnetic moments (in μ_B) as a function of lattice parameter (in a.u.) at Fe and Ru sites for the $RuFe_3N$ nitride.

these atoms and N atoms are more subtle and weak. The interactions between *s* and *p* Ru states with *p* N states appear as a small structure in the *s*- and *p*-DOS at Ru sites at energy range of 0.20–0.50 Ry, which is the energy range where the *p*-DOS at N sites is located (Fig. 2). The formation of magnetic moments out of completely dislocated electrons at Ru and Fe sites is easily explained with the aid of the *d*-DOS. In Figs. 3 and 4, it is seen that for these sites the spin-up *d* states are fully occupied and that some of the spin-down *d* states are empty. Thus, there is a common *d*-band for spin-up electrons, although spin-down electrons are partially excluded from ruthenium and iron sites, which gives the calculated magnetic moment for each site (Table 2). These general features of *l*-DOS at various sites were also reported earlier [10,15,17–21,28] and indicate the metallic character (itinerant electrons) of $RuFe_3N$ and other iron-substituted nitrides, that is, the use of ionic and covalent models are not appropriate to give a good description of their electronic structures.

Table 2 shows the calculated hyperfine fields (H_{FC} the Fermi contact contribution) and isomers shifts (IS) of the $RuFe_3N$. The IS was calculated by using the standard value [40] for the density of the *s*-electrons in the core of the source. The experimental value of H_{FC} at FeII sites (face-centered positions) of Fe_4N nitride is −217 kG [10], while the LMTO theoretical value is −245 kG [10] and FPLAPW theoretical values are −241 kG [20] and −185 kG [34]. The value of H_{FC} decreases to −212 kG in the $Fe_{0.8}Ru_{0.2}Fe_3N$ nitride [7]. This is clearly shown in Table 2 where the LMTO value for H_{FC} at Fe sites agrees with the experiment and with the recent FPLAPW results as well as the calculated value of H_{FC}, which is −134 kG [20].

In order to investigate the sensitivity of magnetic moments against lattice spacing for the $RuFe_3N$ nitride, the magnetic moment was calculated for several lattice parameters simulating pressure effects. Fig. 5 shows the behavior of the magnetic moments at Fe and Ru sites as a function of the lattice spacing. As it can be seen, the LMTO calculations predict that for the $RuFe_3N$ nitride, the magnetic moment at Ru and Fe sublattices decreases to low volumes (higher pressures) with a collapse of the magnetic moment at certain critical lattice spacing. The LMTO results have a sudden drop in the magnetic moment showing that this system has a transition from ferromagnetic state to a nonmagnetic state at low volume, coming to agree with the FPLAPW results on $RuFe_3N$ [20], which also show a collapse of the magnetic moment at low volume. This transition was also observed in other substituted iron nitrides [15,18,19,34,36,37,39] that have an Invar-like behavior as shown by experimental results on thermal expansion, forced magnetostriction [30,32], and applied pressure Mössbauer spectroscopy [31]. The predicted LMTO value for the critical pressure given in Table 1 – close to the values found for other substituted iron nitrides – is another fact as it demonstrates that $RuFe_3N$ has magneto-elastic effects, which is a feature of an Invar-like material.

Our theoretical results also indicate a strong dependence of H_{FC} and IS on the lattice spacing of $RuFe_3N$ as shown in Fig. 6 where the values of H_{FC} (absolute values) and IS at Fe sites are plotted against lattice spacing. The decrease of the absolute value in H_{FC} may be related to the reduction of the contribution on localized *s*-electrons to the spin density at iron nuclei. This behavior of H_{FC} and IS at Fe sites that shrinks the lattice spacing is very similar to that of gold and silver substitution [15] as well as other metallic substitution in Fe_4N and it agrees with the FPLAPW results of Paduani [20]. The calculated value of IS at equilibrium volume given in Table 2 (IS = 0.502 mm/s) is greater than the IS value at face-centered Fe in Fe_4N, where experimental and theoretical values are 0.250 and 0.390 mm/s [10]. In Fig. 6, it can be observed that the reduction of IS value when Ru atoms are substituted by Fe atoms and viewed as a simulation of an applied pressure in $RuFe_3N$ since an increase of *s*-electrons is equivalent to a reduction of *d*-electrons on the IS value. The increase in the density of the *s*-electrons at a low-volume nuclei correlates well with previous DVM calculations [36] on γ'-Fe_4N.

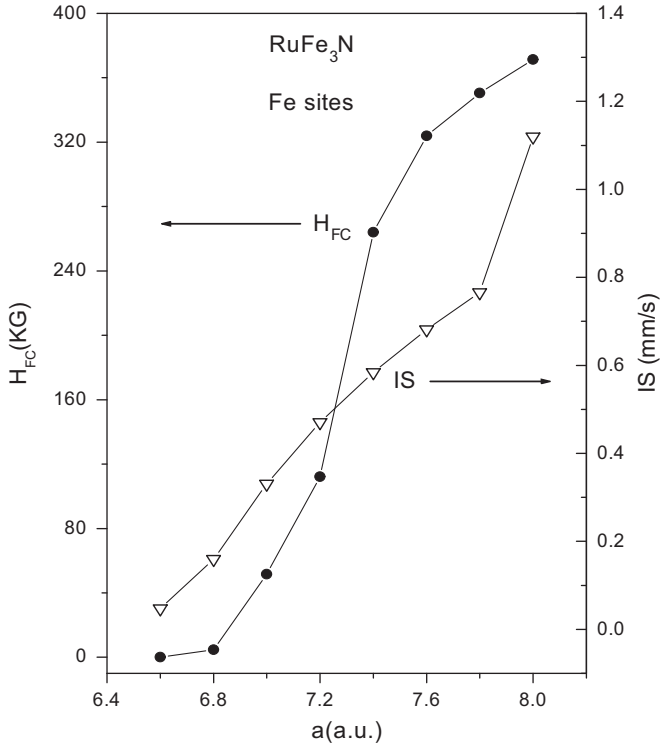

Fig. 6. The hyperfine field (in kG) and the isomer shift (in mm/s) as a function of lattice parameter (in atomic units) at Fe sites of the $RuFe_3N$ nitride.

3. Conclusions

The electronic structure of fully ordered $RuFe_3N$ nitride was studied using the LMTO methods. The LMTO nonmagnetic and ferromagnetic total energy calculations give the equilibrium lattice parameter for this compound in each phase showing that the ferromagnetic is the stable phase, that is, $RuFe_3N$ exhibits ferromagnetic order with local magnetic moments of 1.25 μ_B at ruthenium sites and 1.63 μ_B at iron sites and null magnetic moment at nitrogen sites according to magnetic measurements in $Fe_{0.8}Ru_{0.2}Fe_3N$. For Fe and Ru atoms, the net magnetic moment comes from the low occupation number of spin-down *d*-electrons. The analysis of the density of states shows that the general features of the DOS at Fe and Ru and N atoms are very similar to those that occur in other substituted iron nitrides, and that nitrogen interacts more strongly with Fe at face-centered positions with very small interaction with Ru at corner positions. The calculated magnetic moments and hyperfine parameters at Ru and Fe sites as a function of the lattice parameter showed that $RuFe_3N$ go through a transition from a ferromagnetic to a nonmagnetic state at low volumes (high pressures). Therefore, the magnetism in $RuFe_3N$ is sensitive to the volume, which along with the calculated value of critical pressure, indicates that this nitride shows an Invar-like behavior.

Acknowledgments

We would like to thank the Centro Nacional de Supercomputaç ão (CESUP – UFRGS) for the use of the Cray Supercomputer.

References

[1] M. Abdellaoui, E. Gaffet, Acta Metall. Mater. 43 (1995) 1087.
[2] M. Tier, A. Bloyce, T. Bell, T. Strohaecker. The wear of plasma nitrided high speed steel, in: 11th Conference on Surface Modification Technologies SMT11, Paris, 8–10 September 1997, pp. 887–897.
[3] H. Huang, P.G. McCormick, J. Alloys Compd. 256 (1997) 258.
[4] N. Saegusa, T. Tsukagoshi, E. Kita, A. Tasaki, IEEE Trans. Magn. 19 (1983) 1629.
[5] D. Andriamandroso, L. Fefilatiev, G. Demazeau, L. Fournes, M. Pouchard, Mater. Res. Bull. 19 (1984) 1187.
[6] B. Siberchicot, S.F. Matar, L. Fournès, G. Demazeau, P. Hagenmuller, Eur. J. Solid State Chem. 84 (1990) 10.
[7] D. Andriamandroso, S. Matar, G. Demazeau, L. Fournès, IEEE Trans. Magn. 29 (1993) 2.
[8] M. Kume, S. Takahashi, T. Tsujioka, K. Matsuura, Y. Abe, IEEE Trans. Magn. 24 (1988) 3003.
[9] C. Cordier-Robert, J. Foct, Eur. J. Solid State Inorg. Chem. 29 (1992) 39.
[10] C.A. Kuhnen, R.S. de Figueiredo, V. Drago, E.Z. Da silva, J. Magn. Magn. Mater. 111 (1992) 95.
[11] G. Gao, W.D. Doyle, M. Shamsuzzoha, J. Appl. Phys. 73 (1993) 6579.
[12] J.M.D. Coey, K. O'Donnell, Q. Qiniam, E. Touchais, K.H. Jack, J. Phys.: Condens. Matter 6 (1994) L23.
[13] J. Foct, R.S. de Figueiredo, O. Richard, J.P. Mormiroli, Mater. Sci. Forum 225–227 (1996) 409.
[14] R.S. de Figueiredo, J. Foct, in: Proceedings of ICAME-95, Rimini, Italy, vol. 50, 1996, p. 509.
[15] R.S. de Figueiredo, C.A. Kuhnen, A.V. dos Santos, J. Magn. Magn. Mater. 173 (1997) 141.
[16] R.S. de Figueiredo, J. Foct, M.B.A. de Araújo, Hyperfine Interact. 2 (C) (1997) 235.
[17] C.A. Kuhnen, R.S. de Figueiredo, A.V. dos Santos, J. Magn. Magn. Mater. 219 (2000) 58.
[18] R.S. de Figueiredo, J. Foct, A.V. dos Santos, C.A. Kuhnen, J. Alloys Compd. 315 (2001) 42.
[19] A.V. dos Santos, C.A. Kuhnen, J. Alloys Compd. 321 (2001) 60;
C.A. Kuhnen, A.V. Dos Santos, J. Alloys Compd. 384 (2004) 80.
[20] C. Paduani, J. Magn. Magn. Mater. 278 (2004) 231.
[21] A.V. dos Santos, J.C. Krause, C.A. Kuhnen, Physica B 382 (2006) 290.
[22] O.K. Andersen, Phys. Rev. B 12 (1975) 3060.
[23] H.L. Skriver, in: The LMTO Method: Muffin-Tin Orbitals and Electronic Structure, Springer, New York, 1984.
[24] S.H. Vosko, L. Wilk, M. Nusair, Can. J. Phys. 58 (1980) 1200.
[25] L. Hedin, B.I. Lundqvist, J. Phys. C4 (1971) 2064.
[26] P. Mohn, K. Schwarz, D. Wagner, Phys. Rev. B 43 (1991) 3318.
[27] P. Mohn, K. Schwarz, S. Matar, G. Demazeau, Phys. Rev. B 45 (1992) 4000.
[28] A.V. dos Santos, C.A. Kuhnen, Solid State Commun. 95 (1995) 537;
A.V. dos Santos, C.A. Kuhnen, J. Magn. Magn. Matter 184 (1998) 293;
A.V. dos Santos, C.A. Kuhnen, Thin Solid Films 350 (1999) 258.
[29] C.A. Kuhnen, A.V. dos Santos, J. Alloys Compd. 297 (2000) 68.
[30] S.F. Matar, G. Demazeau, P. Hagenmuller, J.G.M. Armitage, P.C Riedi, Eur. J. Solid State Inorg. Chem. 26 (1989) 517.
[31] J.S. Lord, J.G.M. Armitage, P.C Riedi, S.F. Matar, G. Demazeau, J. Phys.: Condens. Mater. 6 (1994) 1779;
C.L. Yang, M.M. Abd-Elmeguid, H. Micklitz, in: ICAME-95, Rimini, Italy, 1995.
[32] C.L. Yang, M.M. Abd-Elmeguid, H. Micklitz, G. Michels, J.W. Otto, Y. Kong D.S. Xue, F.S. Li, J. Magn. Magn. Mater. 151 (1995) L19.
[33] V.L. Moruzzi, P.M. Marcus, Phys. Rev. B 45 (1992) 2934.
[34] P. Mohn, S.F. Matar, J. Magn. Magn. Mater. 191 (1999) 234.
[35] G.W. Wiener, J.A. Berger, J. Met. 7 (1955) 360.
[36] C. Paduani, J.C. Krause, J. Magn. Magn. Mater. 138 (1994) 109.
[37] C.A. Kuhnen, A.V. dos Santos, J. Magn. Magn. Mater. 130 (1994) 353.
[38] R. Juza, in: H.J. Emeléus, A.G. Sharpe (Eds.), Advances in Inorganic Chemistry and Radiochemistry, vol. 9, Academic Press, New York, 1966, p. 81.
[39] C.A. Kuhnen, A.V. dos Santos, Solid State Commun. 85 (1993) 273.
[40] G. Longworth, Mössbauer Spectroscopy Applied to Inorganic Chemistry, Vol. 1, Plenum Press, London, 1984 (Chapter 4).